15TH IEA HEAT PUMP CONFERENCE
MAY 26–29, 2026 | HOFBURG
VIENNA 2026
DECARBONISATION THROUGH INNOVATION

Pilot Implementation of Cost-Optimized Control for Collective Residential Heat Pumps with Thermal Buffers

E.P. Bontekoe[a,b], W.G. Planje[c], R. van Breukelen[c], F.N. Claessen[d], O. Brouwer[a], I. Lampropoulos[b], W.G.J.H.M. van Sark[b]

[a]Inside-Out Technologies, Tennesseedreef 15b, 3565 CK Utrecht, Netherlands
[b]Utrecht University, Princetonlaan 8a, 3584 CB Utrecht, Netherlands
[c]HU-University of Applied Sciences, Padualaan 99, 3584VC Utrecht, Netherlands
[d]Seita, Asterweg 20N, 1031HN Amsterdam, Netherlands

Abstract

High-rise residential buildings represent a key target for decarbonization, yet electrification of heating via heat pumps can exacerbate local grid congestion. Thermal buffers act as flexible energy storage, allowing heat pumps to shift electricity consumption to cost-effective or low-demand periods while maintaining indoor comfort. This study investigates two complementary approaches for managing thermal buffers in high-rise apartments, with both methods focused on optimized operation: a white-box, rule-based model using model-predictive control (MPC) in a fully virtual simulation, and a solver-based, black-box optimization implemented at a pilot site via the FlexMeasures (FM) platform.

The white-box model employs an Energy Flow-Based Model (EFBM) to simulate heat pump, thermal buffer, PV, electrical battery, and grid interactions under varying weather, occupancy, and electricity price conditions. A Breadth-First Search MPC explores hourly control trajectories over a 36-hour horizon, optimising buffer pre-charging and battery usage to minimize operational cost.

At the pilot site, FM optimization focuses on the thermal buffer as the primary flexibility asset. The Foxtrot BEMS collects real-time measurements, including buffer state-of-charge (SoC), heat pump energy use, building load, PV generation, and ambient conditions, and communicates with FM every 15 minutes. FM returns optimized charging setpoints, which are translated into local heat pump operation while respecting operational constraints and comfort limits.

The results presented here constitute the first experimental exploration that will support a subsequent comparison of the two optimization approaches. Both methods successfully shift buffer charging to cost-effective periods, with the white-box model providing transparent, interpretable insights and FM demonstrating real-world adaptive scheduling under multi-objective constraints. This work lays the groundwork for a larger, ongoing study to systematically evaluate which approach (or hybrid combination) provides the most effective, scalable, and grid-aware control of thermal buffers in high-rise residential heating systems.

Keywords: Building Energy Management System (BEMS); FlexMeasures; thermal energy storage; heat pump; predictive control; price-based scheduling; energy flexibility; self-learning control; demand response; renewable integration;.

1. Introduction

The European Union aims to achieve climate neutrality by 2050 under the European Green Deal, with the Renovation Wave Strategy targeting a doubling of annual renovation rates to decarbonize Europe's building stock [1]. Buildings currently account for nearly 40% of total energy consumption and 36% of CO_2 emissions in the EU [2], and high-rise residential buildings represent both a pressing challenge and a major opportunity for large-scale decarbonization. Recent projects have demonstrated that such buildings can be transformed into sustainable, energy-neutral, or even energy-positive facilities [3][4][5], with the thermal energy system for heating and cooling playing a pivotal role in determining building performance and long-term energy affordability. Electrification of heating through heat pumps, however, can increase local grid congestion, particularly in dense urban areas with limited electrical infrastructure [2][6][7], highlighting the importance of multi-family buildings functioning as local energy hubs that integrate collective heating and cooling installations, on-site photovoltaic (PV) generation, and thermal storage under a Building Energy Management System (BEMS)[8][9].

Thermal buffers in between the building and the heat pump system, function as thermal batteries, and allow heat pumps to shift electricity consumption away from high-demand or high-price periods, improving both operational efficiency and grid compatibility. Instead of storing electricity in electrochemical batteries to subsequently drive heat pumps, energy can be stored directly in thermal buffers, offering a spatially efficient and cost-effective option for buildings with substantial heating and cooling demand. [10][11]. To fully leverage this flexibility, predictive control is interesting to explore: dynamic scheduling of buffer charging and discharging based on expected weather, occupancy, and electricity prices maximizes operational efficiency while reducing grid impact.

This study investigates two complementary approaches for managing thermal buffers in high-rise apartment buildings. First, a white-box, rule-based model is applied, including physics-based relationships and MPC to provide transparent, interpretable, and deployable strategies for scheduling heat pump operation and buffer usage. This approach emphasizes comprehension, adaptability, and practical implementation on modest hardware, such as the Foxtrot BEMS, a building energy management system developed by Inside Out Technologies [12]. Second, a black-box methodology based on FlexMeasures (FM) is examined, which uses optimization engines to automatically compute schedules from forecasts, historical profiles, and multi-objective constraints, enabling fine-grained coordination of heating, PV generation, and storage [13].

This project combines a white-box modelling approach with predictive control principles and insights from solver-based optimization to identify an optimal balance between performance, transparency, flexibility, and scalability in collective residential heating systems. The presented study here represents a first systematic step toward exploring these two approaches, assessing their respective strengths and limitations in delivering reliable, cost-effective, and grid-aware heat to apartment buildings. By documenting this and do initial comparisons, the work establishes a foundation for future research on how white-box and solver-based methods can most effectively leverage thermal storage in high-rise residential applications. Section 2 outlines the methodology used to prepare the analysis. Sections 3 and 4 present and discuss the initial results from both the model and the pilot study, and Section 5 concludes the paper.

2. Methodology

The methodology focuses on comparing two complementary approaches for managing thermal buffers in high-rise residential buildings: a white-box, rule-based model developed entirely in a virtual simulation context, and a solver-based, black-box optimization approach implemented at a pilot site using the FM platform. In both approaches, the thermal buffer in combination with the heat pump serves as the central flexibility asset, enabling the investigation of predictive control strategies and operational optimization.

2.1. White-box model development and predictive control concept

Prior to the pilot implementation, a white-box modelling study was conducted to evaluate the potential of predictive control in heat pump–based building energy systems. A Breadth-First Search–based Model Predictive Controller (BFS-MPC) was implemented within a virtual Building Energy System (BES) represented as a digital twin. The system included a heat pump (HP), thermal buffers for space heating and domestic hot water (DHW), a photovoltaic (PV) system, an electrical battery, and a power grid interface. The digital twin was developed as an Energy Flow-Based Model (EFBM), allowing detailed simulation of thermodynamic behaviour under varying weather conditions, user demand, and hourly electricity market prices from the European Power Exchange (EPEX).

The BFS-MPC performed hourly forward-looking optimization over a 36-hour prediction horizon, systematically exploring control trajectories that combined buffer pre-heating and battery pre-charging to minimize operational cost. This fully virtual implementation allowed the exploration of operational strategies, testing of boundary conditions, and assessment of system sensitivity to occupancy and weather variations without risk to physical hardware. The white-box model provides transparency and interpretability, giving insight into how predictive control interacts with thermal buffer dynamics and heat pump operation, and enabling the evaluation of different control scenarios in a controlled simulation environment.

2.2. Pilot setup with thermal-buffer–focused FM optimization

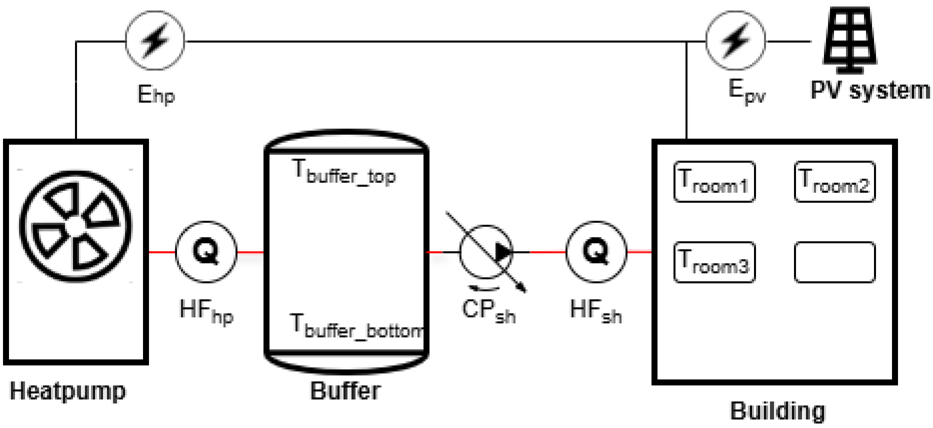

Figure 1 Schematic representation of the experimental heat pump system monitored by the BEMS. The system includes a heat pump, a buffer vessel, and a building with three temperature zones. Electrical meters (E_{hp}, P_{hp}) and (E_{pv}, P_{pv}) measure cumulative energy and instantaneous power for the heat pump and PV system, respectively. Heat flow meters (HF_{hp}, HF_{sh}) monitor thermal energy transfer from the heat pump to the buffer (Q_{hp}) and from the buffer to the space-heating circuit (Q_{sh}). The BEMS uses measurements of buffer and room temperatures (T_{buffer}, T_{room}) and pump status (CP_{sh}) for control and performance evaluation.

At a pilot site, the FM-based approach was implemented with the thermal buffer as the central flexibility asset. The optimization objective could be defined in multiple ways, including minimizing operational cost, maximizing local self-consumption of renewable energy, reducing grid overload, or minimizing CO_2 emissions; in this study, operational cost minimization was prioritized. The pilot setup took place in an office building with a thermal load comparable to the space-heating demand of four apartments. A schematic representation of the setup is represented in Fig 1. Because on-site domestic hot water demand was negligible, only space heating was tested and no DHW buffer was included. The building itself had no PV installation, but a 5 kWp external PV system was connected via an API to emulate local renewable generation (E_{pv}). The setup consisted of a heat pump connected via a heat and flow meter (HF_{hp}), measuring heat produced by the HP (Q_{hp}), which was delivered to a 1000-liter thermal buffer with temperature measurements in top ($T_{buffer,top}$) and bottom ($T_{buffer,bottom}$). HF_{sh} measured the building demand (Q_{sh}) of the test building equipped with low-temperature heat emitters temperature sensors ($T_{room,\ 1\text{-}3}$) and a circulation pump (CP_{sh}) connecting the thermal buffer to the building heating circuit, which was controlled on indoor temperature feedback and a predefined heating schedule. All components were monitored and coordinated by the Foxtrot BEMS, which stored measurement data, and exchanged schedules and forecasts with FM to enable predictive, price-based control (Fig. 2).

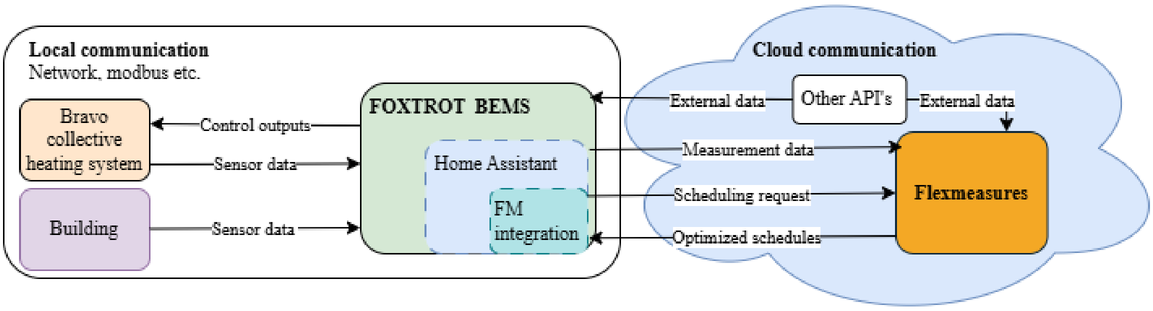

Figure 2 System architecture schematic showing data communication within the pilot. The BEMS controls the collective heating system and reads sensor data through local communication protocols. Communication with FM and other API's takes place over the internet.

Fig. 2 shows that the Foxtrot BEMS (green box) is built on the open-source Home Assistant platform [13]. It handles all local control loops and communicates with sensors and Bravo via Modbus and the local network. Bravo is a collective heating system integrating heat pumps, thermal buffer storage, and hydraulic control components, developed by Inside Out Technologies [15]. The control loops are designed to operate fully offline, ensuring uninterrupted operation even if external services like FM are temporarily unavailable. Locally, the BEMS collects and filters sensor data, stores operational records, generates reports, and exposes key variables for heating-system control. The BEMS operates fully autonomously during normal conditions. The system activates the heat pump when the average buffer temperature $T_{buffer,avg}$ drops below $T_{\min}$ and continues heating until $T_{buffer,avg}$ exceeds $T_{\max}$.

The BEMS communicates with FM (yellow box on the right in fig. 2) through a dedicated HA integration, enabling two-way communication with FM's API. Measurement data was posted every 15 minutes to the FM server. This included cumulative measurements of heat production Q_{hp} and space heating demand Q_{sh}, heat pump electricity demand E_{hp}, PV production E_{pv}. Further on current ambient temperature T_{ext}, buffer temperature $T_{buffer,avg}$ and the ambient temperature forecast were sent. FM handled post-processing of this sensor data: a) snapping cumulative measurements to a fixed 5-minute resolution, b) converting cumulative meter readings into instantaneous power values, and c) computing the actual COP based on Q_{hp} and E_{hp}. This data was then used to generate forecasts for the SoC usage sensor (representing Q_{sh}), E_{PV} and COP. Every five minutes, a scheduling request was sent, providing the current buffer state of charge and a flex-model describing system limits (power capacity, expected demand, dynamic SoC boundaries, storage efficiency, and COP-based charging efficiency). Based on this information, together with its continuously updated internal forecasts, FM produced an optimized power trajectory $P_{set}(t)$ for the upcoming 24 hours at 15-minute resolution. The use of forecasted quantities—such as expected heat demand, COP, and buffer losses—already introduces a degree of self-calibration into the control loop. As these forecasts become more accurate over time, the system effectively begins to adjust its own parameters, laying the foundation for a self-learning and progressively self-optimising control strategy. Due to technical constraints of the heat pump used in the pilot, only on-off operation was possible, therefore a power threshold of 4.5 kW was defined for P_{set}, enabling the FM optimization signal only to influence the control logic by modifying $T_{\min}$ and $T_{\max}$ accordingly. In this way it enabled testing of optimized control strategies based on EPEX electricity prices, PV yield, and weather forecasts via the FM methodology.

3. Results and discussion

The white as well as the black-box model was tested and illustrated *in four contexts*: the **SoC schedules**, **thermal-buffer temperatures**, **heat-pump energy use**, and **indoor climate temperatures**. These examples show how control mechanisms might operate in practice and represent the first exploratory tests of the two model frameworks.

3.1. Conventional Control with the white model

Fig. 3 shows the results of a simulation of the virtual BES under conventional control according to the white model. The indoor temperature (top) stays within its thresholds, while the domestic hot water and space-heating buffers (middle) are charged whenever the lower temperature limit is reached. With both thermal buffers sized large enough to store the next 24 hours of heat demand, early charging of the electrical battery is unnecessary. The bottom plot shows the dynamic electricity rate. This conventional control behaviour—reactive, threshold-based, and non-anticipatory—serves as a baseline for comparison.

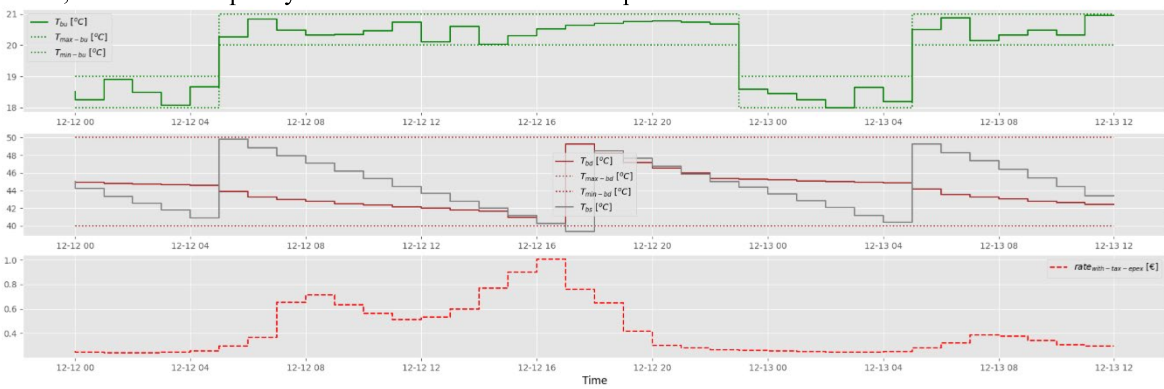

Figure 3 Result of simulation of a conventional controlled virtual BES. Top: indoor temperature (T_{bu}) and set thresholds, middle: temperatures of the domestic hot water thermal buffer (T_{bd}) and the space heating thermal buffer (T_{bs}), bottom: dynamical electrical energy rate (including tax).

Fig. 4 presents the same BES operated with BFS-MPC. Here, both thermal buffers are charged predominantly during cost-effective hours. On the illustrated day, charging shifts to the period between midnight and 06:00, when EPEX prices are lowest. This confirms the model's ability to use predictive information to reduce operating cost. These simulations provided early theoretical validation of predictive control, forming the conceptual foundation for the subsequent FM pilot.

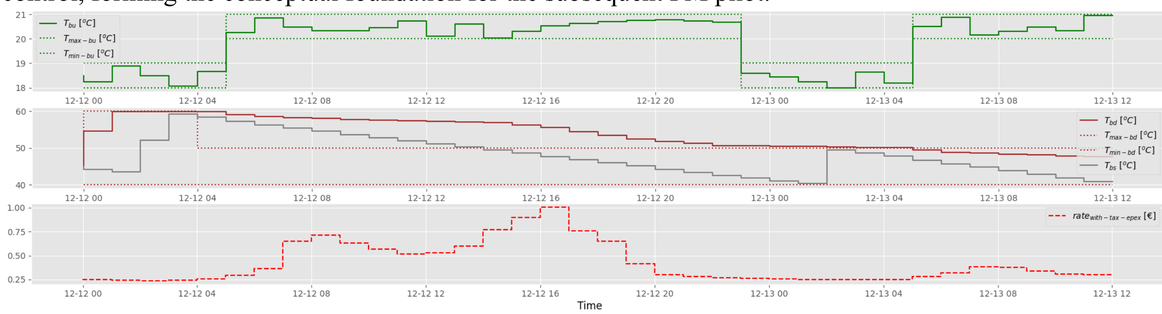

Figure 4. Result of simulation of a BFS-MPC controlled virtual BES. Top: indoor temperature (T_{bu}) and set thresholds, middle: temperatures of the domestic hot water thermal buffer (T_{bd}) and the space heating thermal buffer (T_{bs}), bottom: dynamical electrical energy rate (including tax).

3.2. Interaction Between FM Scheduling, Buffer Dynamics, and Local Heat-Pump Operation

Figs. 5–8 illustrate how FM scheduling, local BEMS logic, heat-pump behaviour, and the building responded during a two-day pilot replay.

Fig. 5 shows the sequence of FM scheduling as day-ahead prices became available. When Friday's prices were published on Thursday afternoon, the optimizer immediately shifted most heating to the cheaper period after midnight. The resulting schedule largely avoided Thursday evening operation, except for small activations compensating for standing losses. However, when the buffer SoC reached its lower limit around 22:00, the local controller activated the heat pump and charged the buffer fully, despite FM scheduling only a short activation window. This occurred because the heat pump's limited modulation—essentially on–off—forces each cycle to continue until T_{max} is reached (further illustrated in Fig. 7). Thus, the interaction reveals a characteristic mismatch between optimized and realized behaviour.

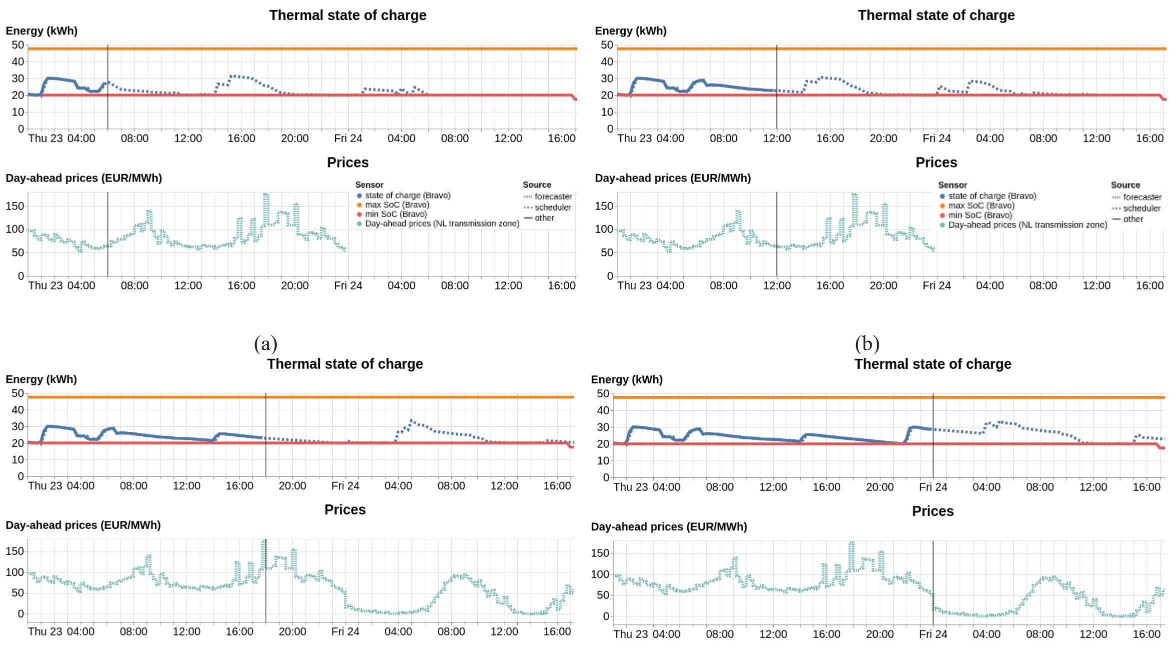

Figure 5 Replay of FM scheduling and local control behaviour over two days. Panels (a–d) show the evolution of the state of charge (SoC, top subplots) and corresponding 15-minute day-ahead electricity prices (bottom subplots), as the schedule was replayed in six-hour increments across Thursday and Friday. The vertical black ruler indicates the current time within each replay snapshot. (a) 6 AM Thursday: the heating buffer just finished charging during cheap early-morning hours. Due to higher standing losses when full, the schedule stays nearer to the SoC minima. (b) Noon Thursday: the schedules plan ahead by 24 hours. Without any price forecasts for Friday, the expected schedule changes only due to changes in the forecast soc-usage. (c) 6 PM Thursday: Friday's day-ahead prices become available, revealing significantly lower prices after midnight. The schedule shows that most heating has been postponed to the cheaper period, while SoC continues to decline gradually. (d) Midnight Friday: the local controller fully charges the buffer even though FM scheduled only a brief activation, illustrating a mismatch between FM control and the local charging logic.

Fig. 6 shows how these scheduling events appeared in the buffer temperatures. Throughout the period, the average buffer temperature $T_{buffer,avg}$ remained between the dynamic limits T_{min} and T_{max}, demonstrating stable control. Only brief stratification occurred after charging events. Around 22:00 on 23 October, the buffer again reached T_{min}, triggering a charging cycle consistent with the SoC behaviour in Fig 5.

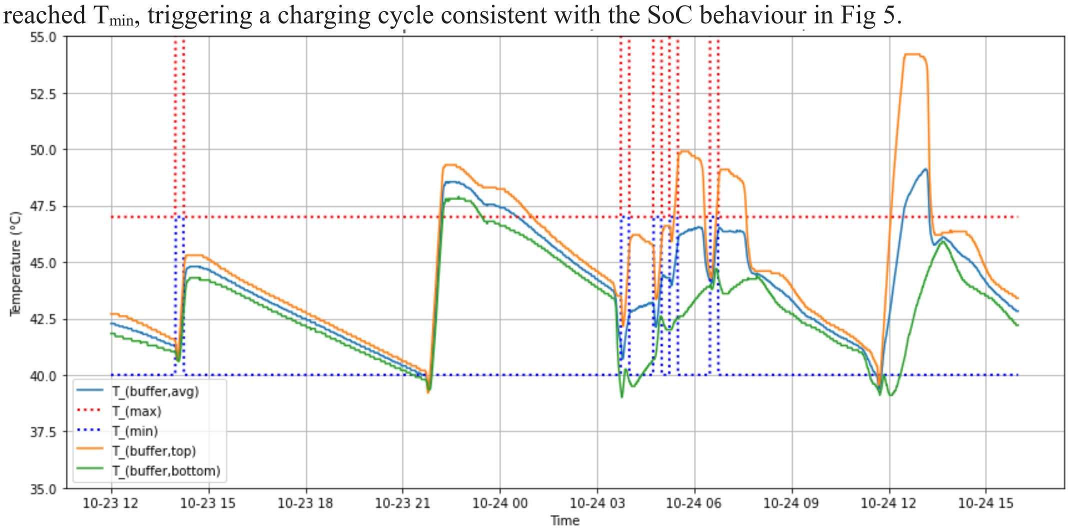

Figure 6 Evolution of buffer temperatures between 23 October 12:00 and 24 October 16:00. The plot shows the measured temperatures at the top ($T_{buffer,top}$) and bottom ($T_{buffer,bottom}$) of the buffer, the spatially averaged buffer temperature ($T_{buffer,avg}$) and the variable minimum and maximum setpoint temperatures (T_{min}, T_{max}; blue and red dotted lines) controlled by the BEMS through the FM signal. Throughout most of the observation period, ($T_{buffer,avg}$) remains within the dynamic setpoint range, indicating stable control behaviour and effective modulation of the heat-pump operation. The small temperature difference between $T_{buffer,top}$ and $T_{buffer,bottom}$ suggests strong thermal mixing within the buffer, with brief periods of stratification visible immediately after heating events when high-temperature supply water enters the tank. Around 22:00 on 23 October, the $T_{buffer,avg}$ dropped to T_{min}, triggering heat-pump activation. The unit subsequently charged the buffer until T_{max} was reached, at which point the compressor switched off.

Fig. 7 compares FM's optimized power signal, the heat pump's actual power consumption, and the day-ahead electricity price. At several moments, the FM signal remained below the ~4.5 kW activation threshold and could not start the heat pump, delaying charging—for example on 24 October around 06:00. Conversely, when the heat pump activated via the T_{min} logic, it continued operating until T_{max} was reached, rather than stopping at the end of the FM-scheduled window. Despite these mismatches, the heat pump still operated mainly during low-price periods, showing that FM's price-driven control successfully shifted most thermal production to economical hours.

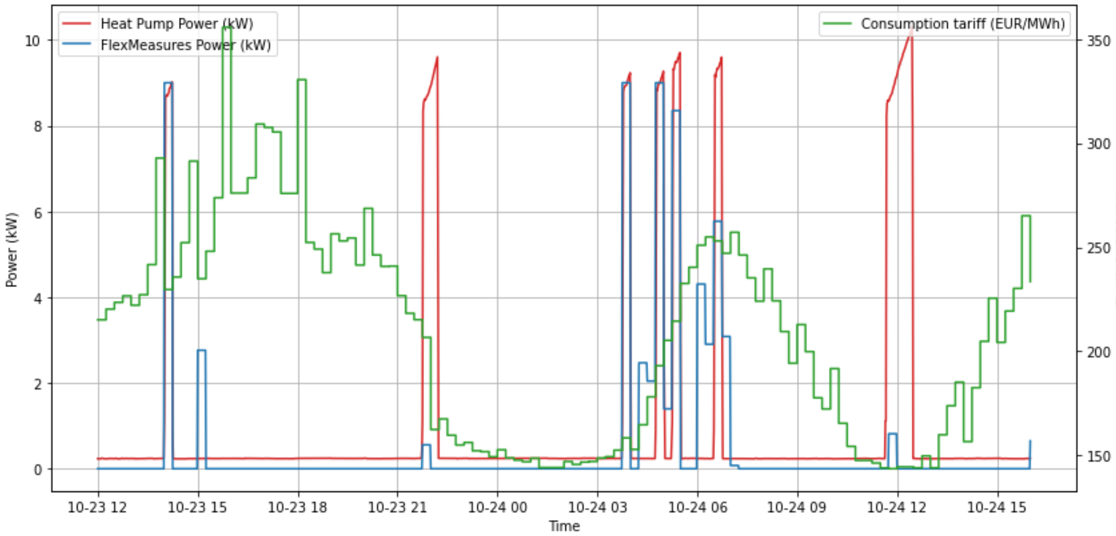

Figure 7. Power consumption of the heat pump (red) and FM control signal (blue) in relation to the day-ahead electricity price (green) between 23 October 12:00 and 24 October 16:00. The FM signal represents the scheduled power demand intended for optimization based on price forecasts, while the actual heat pump power reflects the autonomous control by the BEMS. The figure shows that at several moments the FM power signal remained below the operational threshold required to activate the heat pump. Consequently, heat production continued until the buffer reached T_{max}, rather than ceasing at the end of the FM activation period, or the system ceased to respond. Despite this control mismatch, the timing of heating events closely aligns with low-tariff periods, demonstrating that the price-driven scheduling logic effectively coincided with economical operation.

Fig. 8 shows the indoor temperatures (T_1, T_2, T_3) and the circulation-pump speed. When T_1 and T_2 dropped below ~20 °C, the circulation pump activated and heat was drawn from the buffer; when the temperature thresholds were exceeded, or the scheduled heating period ended, the pump stopped ($RPM_{cp,sh} = 0$). Room temperatures remained mostly within comfort bands, with a temporary overshoot in Room 2 linked to disturbances in Room 1. Room 3, a separate zone, stayed consistently cooler as expected. These results confirm that the FM-driven strategy maintained acceptable indoor conditions while modulating buffer use.

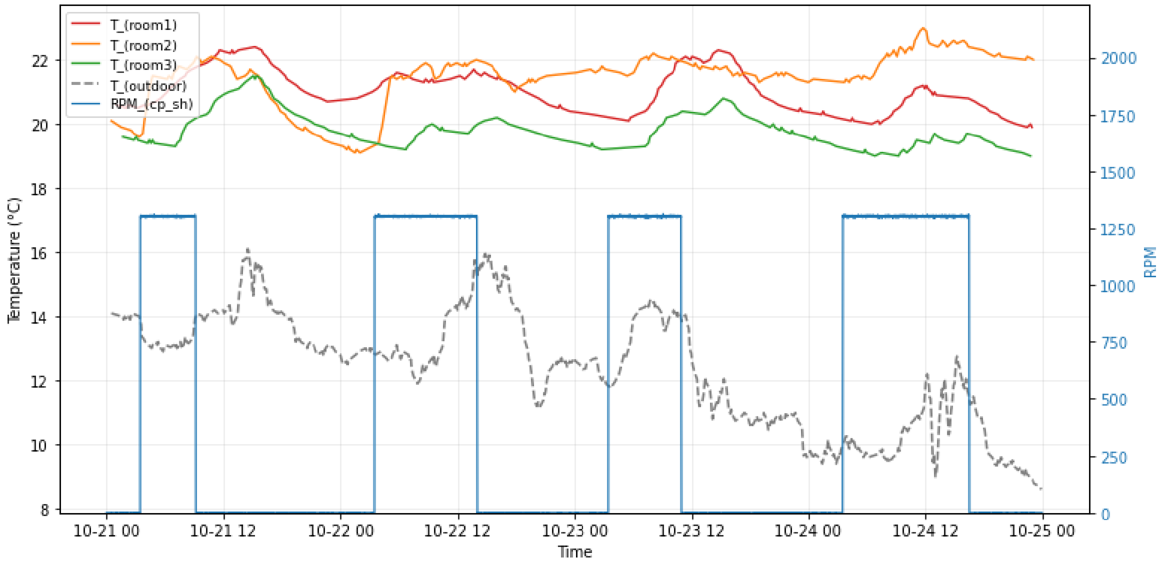

Figure 8 presents the measured indoor temperatures (T_1, T_2, and T_3) and the circulation pump speed (RPM_(cp_sh)) over the observation period. The heating system follows a scheduled operation between approximately 03:30 and 16:30, during which the circulation pump is enabled. When Troom1 and Troom2 fall below 20 °C, the system registers heat demand and the circulation pump activates, initiating heat extraction from the buffer vessel. Conversely, when either Troom1 or Troom2 exceed approximately 22 °C, while the other is above 21.5 °C, or when the scheduled heating period ends, the pump switches off, ceasing buffer discharge.

4. Discussion

This section analyses the performance of the proposed control approach, including the impact of domestic hot water (DHW) integration, temperature safety constraints, and operational limitations identified during the pilot. It examines how modulation capability, thermal buffer capacity, and occupant-level interaction influence system behaviour in a collective heat pump configuration and discusses the implications for scalability and control robustness. The section concludes with a comparative assessment of white-box predictive control and solver-based optimization, highlighting their complementary strengths for design evaluation and real-world operation.

The pilot was conducted in an office building rather than a residential setting. Although the aggregated thermal load is comparable to that of several apartments, user behaviour differs in terms of occupancy patterns and hot water usage was completely excluded. These differences mainly affect demand variability and absolute performance levels. As the analysis focuses on relative control behaviour under comparable boundary conditions, the pilot should be interpreted as a proof of concept of system controllability rather than a direct quantitative comparison with residential operation. Future residential deployments are required for full validation.

Besides space heating demand, the white box model included demand for DHW, which aligns more closely with daytime PV production than space heating. This suggests greater potential benefits from integrating local PV when DHW is actively controlled. Since the field test focused mainly on space heating, this effect could not yet be validated. Future pilots should therefore include DHW to capture this additional flexibility potential. However, the selected timeframe (December) presented in this work exhibited a cost reduction of up to 33% when the controller was applied, illustrating its potential effectiveness even during periods with limited PV generation.

Under conventional control, the white-box model yielded a DHW buffer temperature below 50 °C, which is likely insufficient for Legionella prevention. Although apartment-level electric DHW boosters were assumed, these still require a minimum inlet temperature of approximately 50 °C. Consequently, the modelled configuration underestimates realistic operating temperatures. Enforcing higher DHW buffer temperatures would likely degrade the performance of the conventional control strategy by increasing operating temperatures, thereby amplifying the relative performance advantage of the MPC-based approach through lower COPs and higher electricity consumption. In future work, these temperature constraints should be adapted to ensure safe operation.

In the current control setup, the optimization operates on a 15-minute time resolution, ensuring that the heat pump remains active for at least one control interval. This approach effectively reduces frequent on/off cycling, thereby limiting mechanical wear and extending compressor lifetime [16]. However, further optimization of control sequences may be required to explicitly guarantee lifetime protection, particularly under varying weather conditions and fluctuating heating demand.

A key trade-off exists between runtime duration and operational efficiency. Longer operation at reduced compressor load or lower supply temperatures generally increases the COP and overall system efficiency, whereas short, high-power cycles often lead to greater thermal losses and mechanical stress [17]. Future control strategies should therefore integrate runtime- and efficiency-aware optimization, allowing the BEMS to modulate operation in a way that simultaneously minimizes cost, energy use, and equipment degradation.

During the first pilot, this form of optimization was constrained by limited buffer capacity and the mismatch between building heating demand and the heat pump's modulation range. This limited modulation capability caused several deviations between scheduled and actual operation. FM was designed for generic heat pump applicability where only maximum power could be configured and therefore issues power setpoints assuming finer-grained modulation capability. Because of this, it sometimes scheduled short charging periods or fine-grained ramping, but the heat pump either did not start at all or continued running until $T_{\max}$ was reached. Consequently, the benefits of continuous power-setpoint control—such as smoother operation, reduced cycling, improved COP, and more precise alignment with price or CO_2 signals—could not be fully exploited in this pilot.

Expanding thermal buffer volume and improving modulation capability could enable longer, more stable runtime periods, resulting in higher efficiency and greater operational flexibility [17].

Controlling the circulation pump based on room temperature proved to be a pragmatic approach for reducing distribution losses in the initial pilot setup. However, the results also highlight the vulnerability of such a control strategy: overall system performance can be affected by human intervention, the thermal response characteristics of different heat emitters, and the behaviour of local thermostats. In a full-scale deployment, occupants retain control over indoor temperatures through apartment-level thermostats, preserving user comfort and autonomy. Due to the aggregation of a large number of apartments, individual setpoint adjustments have a limited and effectively averaged impact on the operation of the collective heating system

The central control system should therefore not specifically rely on data from individual apartments. Instead, the main distribution network continuously supplies heat to meet both space-heating and DHW demand, ensuring availability at all times. Indoor temperature measurements will primarily be used to confirm that apartments maintain comfortable under varying weather conditions. This could be used to determine the optimal heating curve, tuning the system to identify the lowest supply temperature at which all apartments still receive sufficient heat delivery, thereby maximizing the SCOP [18].

The pilot was conducted from February to the end of October 2025. The initial phase focused on establishing system connectivity, configuring operational parameters, and collecting sufficient data to estimate heat demand, COP, and PV production. Because outdoor temperatures remained relatively mild for most of the period, opportunities to test the system under sustained low-temperature heating conditions were limited. As a result, the financial benefits of price-based operation could not be fully assessed.

In addition, the self-learning capabilities associated with coupling the BEMS with the FM optimization platform, in which operational data and demand patterns are used to update device parameters such as heat pump efficiency and storage losses, could not be sufficiently evaluated within the scope of the present pilot.

Nevertheless, the results obtained during the available heating moments indicate that the approach has strong potential, and more pronounced advantages are expected during colder periods and over longer operational windows.

Taken together, these results provide a first empirical comparison of white-box predictive control and solver-based optimization for thermal buffers, highlighting their complementary strengths: the white-box model excels in interpretability and scenario testing, while FM provides adaptive, data-driven real-world control.

5. Conclusion and recommendations

This study presents the initial results of an ongoing effort to compare two complementary approaches for optimized control of thermal buffers in high-rise residential buildings: a white-box, rule-based model employing MPC and a solver-based, black-box optimization implemented at a pilot site using the FM platform. In both approaches, the thermal buffer in combination with the heat pump serves as the central flexibility asset, enabling predictive and cost-driven operation while maintaining indoor comfort.

The white-box model demonstrates that predictive optimization can shift buffer charging to periods with low electricity prices, reducing operational costs and improving energy efficiency. Using an EFBM, the white-box MPC provides transparency and interpretability, allowing exploration of “what-if” scenarios, sensitivity analysis under varying occupancy and weather conditions, and risk-free testing of operational strategies in a fully virtual environment.

The FM-based pilot complements this by implementing real-time, solver-based optimization at the building scale. The Foxtrot BEMS transmits measurements including buffer state-of-charge, heat pump energy consumption, building load, PV generation, and ambient conditions every 15 minutes to FM. The platform calculates optimized heat pump setpoints under technical, operational, and comfort constraints, which are locally applied via the BEMS. Early results show that FM successfully shifts most thermal production to cost-effective hours, while maintaining buffer SoC within dynamic limits and ensuring acceptable indoor temperatures. Interactions between scheduled and actual heat pump operation reveal characteristic mismatches due to modulation thresholds, but overall, the system demonstrates adaptive, real-world optimization potential. As operational data accumulates, the combined BEMS–FM setup can increasingly refine its internal forecasts and parameter estimates, enabling a gradual shift toward a self-calibrating, data-driven control strategy that improves performance over time.

This paper represents a foundational step in an ongoing experiment to determine the most effective strategies for smart thermal buffer management, ultimately aiming to integrate predictive control, storage flexibility, and cost-efficient operation in collective heat pump systems across high-rise residential buildings. Future work will extend these findings to longer-term trials, multi-day operation, and hybrid approaches to identify optimal control strategies for large-scale deployment.

Acronyms

API — Application Programming Interface
BEMS — Building Energy Management System
BES — Building Energy System
BFS — Breadth-First Search
DHW — Domestic Hot Water
EFBM— Energy Flow Based Model
EPEX — European Power Exchange
FM — FlexMeasures
HA — Home Assistant
HF — Heat and Flow Meter
HP — Heat Pump
LT — Low-Temperature (heating system)
MPC — Model Predictive Controller
PV — Photovoltaic
RES — Renewable Energy Sources
(S)COP — (Seasonal) Coefficient of Performance
SH — Space Heating
SOC — State of Charge

Acknowledgements

This work was partially supported by the Province of Utrecht through the USET (Uitvoeringsverordening subsidie Energietransitie) programme within the project BEMS4Hoogbouw. We gratefully acknowledge this support, which enabled the development and testing of the modelling framework presented in this study.

References

[1] European Commission. (2020). A Renovation Wave for Europe – Greening our buildings, creating jobs, improving lives. COM(2020) 662 final. Brussels: European Commission. https://eur-lex.europa.eu/legal-content/EN/TXT/?uri=CELEX:52020DC0662

[2] International Energy Agency (IEA). (2023). Net Zero by 2050 – Buildings Sector Pathway. Paris: IEA. https://www.iea.org/reports/net-zero-by-2050

[3] Inside Out. (2025). *Henriëttedreef – Projecten*. Retrieved November 17, 2025, from https://www.inside-out.tech/projecten/henriettedreef

[4] Jiang, D., Zhao, Y., & Chen, H. (2024). Techno-economic analysis of a high-rise residential nearly zero-energy building. Sustainability, 16(15), 6288. https://doi.org/10.3390/su16156288

[5] Coccato, S., Bontekoe, E., Lampropoulos, I., & van Sark, W. (2025) Evaluating Post-Retrofit Energy Performance in a Plus Energy Building: Smart Meter Data Reconstruction and Battery Sizing Insights. Chapter 36 in Sustainability in Energy and Buildings 2025, Smart Innovation, Systems and Technologies 470, (J. Littlewood, L. Jain, R.J. Howlett (Eds), Springer Nature Singapore Pte Ltd., 2026 (in press))

[6] Groenenberg, H. (2025). Driving the Energy Transition in The Face of Grid Congestion. Journal of Earth and Environmental Sciences Research, 1–7. https://doi.org/10.47363/JEESR/2025(7)236

[7] Van Someren, C., Visser, M., & Slootweg, H. (2021). Impacts of electric heat pumps and rooftop solar panels on residential electricity distribution grids. In 2021 IEEE PES Innovative Smart Grid Technologies Europe (ISGT Europe) (pp. 1–6). IEEE. https://doi.org/10.1109/ISGTEurope52324.2021.9640090

[8] Adhikari, S., Nguyen, K., & Wang, L. (2025). A review of smart building energy management systems. EasyChair Preprints. https://easychair.org/publications/paper/1qDQ/open

[9] Balali, Y., Abedi, A., & Fathi, S. (2023). Energy modelling and control of building heating systems in a transitional energy system. Renewable and Sustainable Energy Reviews, 182, 113491. https://doi.org/10.1016/j.rser.2023.113496

[10] IRENA. (2020). *Innovation Outlook: Thermal Energy Storage.* International Renewable Energy Agency.

[11] Oldewurtel, F., Sturzenegger, D., Andersson, G., Morari, M., & Smith, R. S. (2012). *Building energy optimization: Towards automated demand response.* Energy and Buildings, 47, 100–110. https://doi.org/10.1016/j.enbuild.2011.11.021

[12] Inside Out Technologies (2026). *IO-Foxtrot: Data Module, 2025.* https://www.inside-out.tech/modules/io-foxtrot

[13] FlexMeasures. (2025). *FlexMeasures: Open-source energy flexibility platform*. https://flexmeasures.io

[14] Home Assistant. (2025). *Home Assistant: Open-source home automation platform*. https://www.home-assistant.io

[15] Inside Out Technologies (2026). *IO-Bravo: Collective Heating System Module, 2025.* https://www.inside-out.tech/modules/io-bravo

[16] Brüder Müller, T., et al. (2023). *Large-Scale Monitoring of Residential Heat Pump Cycling: Run Times, Frequency, and Influence on Performance*. Applied Thermal Engineering, 233, 119315. https://doi.org/10.1016/j.applthermaleng.2023.119315

[17] Dongellini, M., & Morini, G. L. (2019). *On–off cycling losses of reversible air-to-water heat pump systems as a function of the unit power modulation capacity.* Energy Conversion and Management, 196, 966–978. https://doi.org/10.1016/j.enconman.2019.06.022

[18] Potočnik, P., Vidrih, B., Kitanovski, A., & Govekar, E. (2018). *Analysis and optimization of thermal comfort in residential buildings by means of a weather-controlled air-to-water heat pump.* Building and Environment, 140, 68–79. https://doi.org/10.1016/j.buildenv.2018.05.044